Constraints on continental crustal mass loss via chemical weathering using lithium and its isotopes

Xiao-Ming Liu[1] and Roberta L. Rudnick[1]

Department of Geology, University of Maryland, College Park, MD 20742

This contribution is part of the special series of Inaugural Articles by members of the National Academy of Sciences elected in 2010.

Contributed by Roberta L. Rudnick, November 4, 2011 (sent for review August 2, 2011)

Chemical weathering, as well as physical erosion, changes the composition and shapes the surface of the continental crust. However, the amount of continental material that has been lost over Earth's history due to chemical weathering is poorly constrained. Using a mass balance model for lithium inputs and outputs from the continental crust, we find that the mass of continental crust that has been lost due to chemical weathering is at least 15% of the original mass of the juvenile continental crust, and may be as high as 60%, with a best estimate of approximately 45%. Our results suggest that chemical weathering and subsequent subduction of soluble elements have major impacts on both the mass and the compositional evolution of the continental crust.

arc basalts | lithium isotopes | mass balance modeling | crust composition | chemical weathering rate

It is well established that the average composition of the continental crust is intermediate or "andesitic," if described in terms of an igneous rock type ($SiO_2 = 57 \sim 64$ wt. %) (1 and references therein). However, the magmas that generate the present-day continental crust are dominantly basalt (2 and references therein). This discrepancy has been referred to as the "crust composition paradox" (3). Various hypotheses have been proposed to solve this paradox, including stripping of Mg through chemical weathering (4–6), removal of mafic/ultramafic lower crust through foundering/delamination (7–9), subduction of continental crust followed by "relamination" of buoyant, felsic crust (10), or direct addition of tonalites to the crust through slab melting in a hotter Archean Earth (e.g., 2, 3, 11).

During chemical weathering of the continents, soluble elements (e.g., Na, Ca, Mg, and Li) are dissolved and transported to the oceans via rivers and/or groundwater, while insoluble elements, such as Si and Al, remain in the continental regolith. Ultimately, these soluble components may be recycled into the mantle by subduction (e.g., Mg and Ca, 5) or may reenter continental crust via arc magmatism (e.g., Na). Therefore, chemical weathering may be an important process that controls the mass, the composition and the evolution of the continental crust. However, only one attempt has previously been made to quantify the influence of chemical weathering on the mass and composition of the continental crust (6).

Using a mass balance model coupled with the correlation observed between lithium and magnesium in modern river waters and assumptions regarding the mass lost from the continental crust due to lower crustal recycling, Lee et al. (6) argued that approximately 20% of the juvenile continental crustal mass has been lost from the continental crust due to chemical weathering. However, the Li concentration they used for primitive island arc basalts (15 ppm) is about a factor of two higher than average compositions of arc basalts or other oceanic basalts [e.g., mid-ocean ridge basalts (MORB) or ocean island basalts (OIB) see below]. When using a more accurate concentration (7 ppm), the Mg/Li mass balance becomes untenable, as the proportion of bulk continental crust exceeds one, implying mass addition due to chemical weathering. A fundamental problem is that Li is a moderately incompatible trace element, whose concentration in crustal rocks varies by several orders of magnitude, while Mg, a major element, may vary in concentration by only a factor of two to three. Thus, the Li/Mg ratio is sensitive to the more variable Li concentration. In addition, Li is a trace element whose partitioning may not always follow Mg, and, with newer data (see Dataset S1), it is clear that the Mg/Li ratio in river waters is quite variable, reflecting the influence of factors such as watershed lithology, that influence riverine Mg/Li, in addition to continental weathering.

Here, we explore the utility of using a single soluble element, Li, and its isotopes (^{6}Li and ^{7}Li), to constrain the mass of continental crust lost to weathering, employing a mass balance approach similar to that of Lee et al. (6). While there are a number of assumptions that go into this calculation, giving rise to a family of outcomes, our aim here is not so much to provide the answer regarding the mass of continental crust lost to chemical weathering, but rather, to place limits on this mass.

Lithium Isotopes

Lithium has two stable isotopes with the following relative abundances: ^{6}Li $\sim 7.5\%$ and ^{7}Li $\sim 92.5\%$. Because the mass difference between these two isotopes is relatively large (approximately 16%), they show significant mass dependent fractionation in nature (>50‰) (12), expressed in δ^7Li notation: $\delta^7\text{Li}(‰) = ([^7\text{Li}/^6\text{Li}]_{\text{sample}}/[^7\text{Li}/^6\text{Li}]_{\text{standard}} - 1) \times 1000$, where the standard used is a synthetic Li carbonate, L-SVEC (13). During chemical weathering, secondary minerals, such as clays, take ^{6}Li preferentially into their structure, resulting in heavier Li isotopic composition in rivers and lighter isotopic composition in the regolith (14–22). The lithium concentration and isotopic composition of the continental crust, as well as river waters, are well documented by various authors (17, 19–26). In addition, Li concentration and isotopic composition of potential building blocks of the continental crust, namely, basaltic arc lavas (28–32) and Archean tonalites, trondhjemites, and granodiorites (TTG, 17, 33) are known. Collectively, these studies demonstrate that the δ^7Li of present-day bulk continental crust is 2–3‰ lower than that of its potential building blocks (i.e., mantle-derived basalts), which likely reflects the influence of chemical weathering on the bulk crust composition (17, 24). Therefore, Li and its isotopes may be useful in quantifying the amount of continental crust lost through chemical weathering.

Mass Balance Model

The conceptual model of continental crust recycling is illustrated in Fig. 1, where juvenile arc basalts or felsic slab melts form the input to the crust, and there are three outputs: recycled lower crust (lower crust that is lost from the continents by foundering,

Author contributions: X.-M.L. and R.L.R. designed research; X.-M.L. performed research; X.-M.L. and R.L.R. analyzed data; and X.-M.L. and R.L.R. wrote the paper.

The authors declare no conflict of interest.

[1]To whom correspondence may be addressed. E-mail: xliu1235@umd.edu or rudnick@umd.edu.

This article contains supporting information online at www.pnas.org/lookup/suppl/doi:10.1073/pnas.1115671108/-/DCSupplemental.

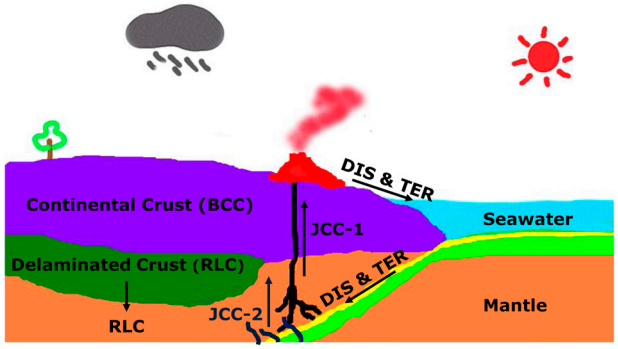

Fig. 1. Cartoon illustrating the mass balance approach used for solving the weathering flux from the continents (DIS). Juvenile crust is created via a JCC magmatic flux from the mantle that produces either a basalt (JCC-1) or felsic slab melts (e.g., in a hotter, Archean Earth) (JCC-2). There are three outputs fluxes from this juvenile crust: recycled lower crust (RLC), soluble components dissolved during weathering (DIS), which wash into the ocean and may be removed by uptake in sea floor sediments and altered basalt, and sediments derived from the continents and removed via subduction (TER). The net result of these input and outputs to the continental crust is the present-day bulk continental crust (BCC).

subduction, or other processes), subducted terrigenous sediments (net output from the continent to the ocean in solid form, transported as the suspended sediments and bed load of rivers), and the crust dissolved and removed from the continents by weathering. The net effect of these processes is a change of the composition of the continental crust, leading to the current bulk continental crust composition.

The following assumptions and definitions are applied (all variables used in this model are defined in Table 1):

1. The continental crust is ultimately derived from juvenile continental crust (JCC), X_i is the mass fraction of each reservoir, BCC is the present-day bulk continental crust, RLC is recycled lower crust, DIS is the mass of crust dissolved during weathering and removed via rivers, TER is terrigenous sediments removed via subduction, and the sum of the mass fraction of each reservoir is one ($X_{BCC}+X_{RLC}+X_{DIS}+X_{TER}=1$).
2. The ^{6}Li and ^{7}Li removed from the continents due to chemical weathering is approximated by their concentration ratios in modern rivers; that is $f^i_{DIS}=f^i_{RIV}$ (f is defined below).

The mass balance model is:

$$C^i_{JCC}=X_{BCC}C^i_{BCC}+X_{RLC}C^i_{RLC}+X_{DIS}C^i_{DIS}+X_{TER}C^i_{TER} \quad [1]$$

where, for an isotope i, the concentration of i in JCC, BCC, RLC, DIS, and TER are C^i_{JCC}, C^i_{BCC}, C^i_{RLC}, C^i_{DIS}, and C^i_{TER}. And X_{BCC}, X_{RLC}, X_{DIS}, and X_{TER} are the mass fractions of BCC, RLC, DIS, and TER relative to JCC, respectively. The fraction of i lost by dissolution is f^i_{DIS}, where $f^i_{DIS}=X_{DIS}\frac{C^i_{DIS}}{C^i_{JCC}}$. For example, we have $f^{7Li}_{DIS}=X_{DIS}\frac{C^{7Li}_{DIS}}{C^{7Li}_{JCC}}$ and $f^{6Li}_{DIS}=X_{DIS}\frac{C^{6Li}_{DIS}}{C^{6Li}_{JCC}}$ for ^{7}Li and ^{6}Li, respectively. Similar definitions are applied for the fraction of i in the present-day bulk continental crust (BCC), recycled lower crust (RLC), and terrigenous sediments removed via subduction (TER). Thus, Eq. **1** becomes

$$f^i_{BCC}+f^i_{RLC}+f^i_{DIS}+f^i_{TER}=1 \quad [2]$$

Rearranging Eqs. **1** and **2**, and substituting ^{7}Li and ^{6}Li for i we have

$$f^{7Li}_{DIS}=1-X_{BCC}\frac{C^{7Li}_{BCC}+R_{RLC/BCC}C^{7Li}_{RLC}+R_{TER/BCC}C^{7Li}_{TER}}{C^{7Li}_{JCC}}$$
$$f^{6Li}_{DIS}=1-X_{BCC}\frac{C^{6Li}_{BCC}+R_{RLC/BCC}C^{6Li}_{RLC}+R_{TER/BCC}C^{6Li}_{TER}}{C^{6Li}_{JCC}} \quad [3]$$

where $R_{RLC/BCC}=X_{RLC}/X_{BCC}$ and $R_{TER/BCC}=X_{TER}/X_{BCC}$. Lithium concentrations and isotopic compositions in different reservoirs, such as those in JCC, BCC, RLC, and TER can be estimated, along with uncertainties, from published data. Therefore, the concentration of ^{7}Li and ^{6}Li in JCC, BCC, RLC, and TER can be calculated based on Li concentration and δ^7Li (correction is made for the difference in molecular weight of ^{7}Li and ^{6}Li). Inputs to the mass balance model are discussed in detail below and summarized in Table 2.

Lithium concentration and isotopic composition in JCC (juvenile continental crust) are discussed in terms of two end-member scenarios: (*i*) the JCC has the same Li concentration and isotopic composition as present-day arc basalts; (*ii*) JCC is a 70:30 mixture of arc basalts and Archean TTG, which have been suggested to result from melting of subducted slabs (27).

In scenario one, we assume that present-day arc basalts are representative of JCC through time. The lithium concentration and isotopic composition in JCC are compiled from literature data for arc basalts ($SiO_2=45\sim55\%$ wt.) (28–32, 34) and the GEOROC database (35). Overall, 552 Li concentrations and 75 δ^7Li values are available, worldwide. Data are compiled in

Table 1. Variables used and their definitions

Variable	Definition
X_{BCC}	mass fraction of the present-day bulk continental crust relative to JCC
X_{RLC}	mass fraction of the recycled lower crust relative to JCC
X_{DIS}	mass fraction of the crust dissolved during chemical weathering and removed via rivers and subduction of altered oceanic crust relative to JCC
X_{TER}	mass fraction of the terrigenous sediments removed via subduction relative to JCC
i	an isotope (either ^{6}Li or ^{7}Li in this study)
C_{JCC}	concentration of i in JCC
C_{BCC}	concentration of i in BCC
C_{RLC}	concentration of i in DLC
C_{DIS}	concentration of i in DIS
C_{RIV}	concentration of i in rivers
C_{TER}	concentration of i in TER
f_{BCC}	fraction of i in BCC relative to JCC
f_{RLC}	fraction of i in RLC relative to JCC
f_{DIS}	fraction of i in DIS relative to JCC
f_{RIV}	fraction of i in rivers relative to JCC
f_{TER}	fraction of i in TER relative to JCC
$R_{RLC/BCC}$	ratio of mass removed by lower crustal recycling (X_{RLC}) compared to BCC (X_{BCC})
$R_{TER/BCC}$	ratio of mass of sediments removed by subduction (X_{TER}) compared to BCC (X_{BCC})

Table 2. Input parameters for mass balance model with sensitivity analysis results for scenarios one and two, and associated change in the amount of crust lost due to weathering (X_{DIS})

Scenario 1: JCC (present-day arc basalt)

	[Li], ppm	Range*	SI†	X_{DIS}range, %	δ^7Li, ‰	Range*	SI†	X_{DIS} range, %
JCC‡	6.9	4.5–10.6	0.48	38–74	3.6	2.4–4.8	0.08	57–62
BCC§	18	11–20	0.20	50–62	1.2	0–4	0.07	57–61
RLC¶	3.5	1.5–8	0.10	58–64	3.6	−7.5–11.5	0.06	58–62
TER‖	48	32–73	0.20	53–67	3	−1.6–5	0.08	58–63
DIS/RIV**	1.5×10^{-3}	–	–	–	23.4	14–28	0.04	59–62
	Best estimate	Range*	SI†	X_{DIS} range, %				
$R_{RLC/BCC}$	1	1.5–4.5	0.57	23–53				
$R_{TER/BCC}$	0.3	0.2–1.1	0.27	53–72				

Scenario 2: JCC (Archean TTG and present-day arc basalt)

	[Li], ppm	Range*	SI†	X_{DIS} range, %	δ^7Li, ‰	Range*	SI†	X_{DIS} range, %
JCC‡	10.2	8–14	0.60	22–56	4	3.4–4.5	0.07	42–45
BCC§	18	11–20	0.34	31–47	1.2	0–4	0.12	40–45
RLC¶	5.1	1.5–8	0.19	38–47	3.6	−7.5–11.5	0.14	41–47
TER‖	48	32–73	0.35	35–53	3	−1.6–5	0.15	41–48
DIS/RIV**	1.5×10^{-3}	–	–	–	23.4	14–28	0.10	43–47
	Best estimate	Range*	SI†	X_{DIS} range, %				
$R_{RLC/BCC}$	1	1.1–3.1	0.67	14–42				
$R_{TER/BCC}$	0.3	0.2–1.1	0.43	34–60				

*All ranges are discussed in text, compilation of [Li] and δ^7Li in JCC for scenario one are shown in Fig. 2*A* and 2*B*; and [Li] and δ^7Li in JCC for scenario two were calculated based on weighted distribution of Archean TTG (Fig. 2*C* and 2*D*) and mean of arc basalts.

†Sensitivity analyses are performed to evaluate the uncertainty on the mass balance model. Sensitivity index, defined as $SI = [X_{max} - X_{min}]/X_{max}$, was calculated for each parameter (50).

‡From the compilation of current arc basalt and Archean TTG data (see Fig. 2).

§From Teng et al. (24) and references therein.

¶The optimal value of [Li] is assumed to be half that of the original crust (JCC), with the same δ^7Li.

‖From Dataset S1 and Chan et al. (43) and references therein.

**World river average from Huh et al. (23).

Dataset S2 and histograms of Li concentration and δ^7Li are plotted in Figs. 2*A* and 2*B*. Lithium concentrations in arc basalts follow a log-normal distribution, having a mean of 6.9 ppm, with a one sigma lower and upper limit of 4.5 ppm and 10.6 ppm, respectively. The δ^7Li of arc basalts follow a normal distribution, with a mean δ^7Li of +3.6‰ and a standard deviation of 1.2. Because arc basalts may contain enhanced Li from subducted terrigeneous sediments or altered oceanic crust, and this Li ultimately derives from weathering of continental crust (e.g., 32), alternative juvenile basaltic additions to the crust that lack such potential crustal input (e.g., MORB and OIB, rather than island arc basalt), and the resulting influence on the mass balance outcome, are discussed below.

In scenario two, we assume that 30% of the JCC is composed of Archean tonalite-trondhjemite-granodiorite (TTG), which may have formed as slab melts, and the remaining 70% is present-day arc basalts (assuming Archean basalts have the same Li compositions as present-day arc basalts). This proportion of TTG derives from estimates of Taylor and McLennan (36), who suggest that 60% of the continental crust formed in the Archean and that this Archean crust is half basalt and half TTG, yielding 30% total TTG in the bulk crust, with the remainder assumed to be arc basalts. This proportion of continental crust formed in the Archean is in agreement with crust preservation curves based on detrital zircon Hf model ages [see (37) and references therein]. Limits on the proportion of TTG in JCC, and its influence on the mass balance outcome, are discussed in the following section.

There are two sources of Li isotopic data for TTG (17, 33). Teng et al. (24) report lithium data for composite Archean TTG from the North China Craton. Qiu (33) reports Li concentration and isotopic compositions for a variety of Archean TTG, which range from inferred juvenile melts (e.g., the "Sanukatoids" of the Superior Craton, 38) to melts of thickened basaltic crust (e.g., TTG of Barberton Mountain Land, South Africa, 39). Because granulite-facies TTG of the Scourian Complex have unusually low Li concentration (3.0 to 12.5 ppm) and highly variable δ^7Li (+0.2‰ to +11.7‰), suggesting that Li was lost and possibly fractionated by deep crustal processes (33), we confine our compilation to TTG that have experienced amphibolite-facies or lower grades of metamorphism. These data are compiled in the Dataset S2, and histograms of Li concentration and δ^7Li of these Archean TTGs are plotted in Figs. 2*C* and 2*D*. Li concentrations of juvenile Archean TTGs follow a log-normal distribution, having a mean of 18 ppm, with an upper limit of 30 ppm and a lower limit of 11 ppm. The δ^7Li of the Archean TTGs are fit to a normal distribution with a mean of +4.3‰ and a standard derivation of 1.0. Using the average Li concentration of 18 ppm, along with its upper and lower limits, we calculate the average Li concentration in the JCC for scenario two is 10 ppm, with a lower and upper limit of 8 ppm and 14 ppm, respectively. Since δ^7Li in Archean TTG show mantle-like values of +4.3‰ ± 1.0 (1σ) (24, 33), we calculate a weighted average δ^7Li of +4.0 for scenario two JCC, with a lower limit of +3.4‰ and an upper limit of +4.5‰.

Li concentration and isotopic composition of the current bulk continental crust (BCC) is 18 ppm and +1.2‰, respectively (24). Because Li is a moderately incompatible element, recycled lower crust, which forms as cumulates or residues, should have a lower concentration than its juvenile parent (JCC). Thus, we assume a Li concentration of either 3.5 ppm or 5.1 ppm for RLC, which is half that of the juvenile continental crust value for scenario one and two, respectively. Such concentrations are similar to or lower than the average Li concentration of the present lower continental crust [8 ppm; (24, 40)]. It is assumed that the Li isotopic composition of RLC is the same as that of JCC, since there is no significant isotopic fractionation during basalt differentiation (41). Li concentration and isotopic composition in TER can

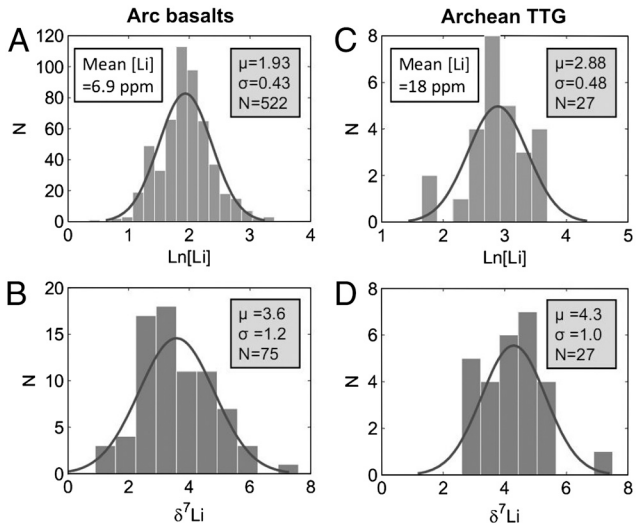

Fig. 2. Histogram of lithium concentrations and isotopic compositions in basaltic arc lavas and Archean TTGs. μ, σ, and N represent mean, standard deviation, and number of the sample population. (*A*) In arc basalts, Li concentration follows a log-normal (natural log) distribution with a mean of 6.9 ppm and upper and lower limits of 10.6 ppm and 4.5 ppm, respectively. (*B*) δ^7Li in arc basalts is fit by a normal distribution curve, with a mean of +3.6 and a standard deviation of 1.2. (*C*) In Archean TTGs, Li concentration follows a log-normal (natural log) distribution with a mean of 18 ppm and upper and lower limits of 30 ppm and 11 ppm, respectively. (*D*) δ^7Li in Archean TTGs is fit by a normal distribution curve, with a mean of +4.3 and a standard deviation of 1.0.

be approximated from the average [Li] and δ^7Li of terrigenous sediments of 48 ppm and +3‰, respectively (Dataset S1 and 43).

Adopting the above values leaves four unknowns in Eq. **3**: f^i_{DIS}, $R_{\mathrm{RLC/BCC}}$, $R_{\mathrm{TER/BCC}}$ and X_{BCC}. In addition, we have

$$\frac{f^{^7\mathrm{Li}}_{\mathrm{DIS}}}{f^{^6\mathrm{Li}}_{\mathrm{DIS}}}=\frac{X_{\mathrm{DIS}}\dfrac{C^{^7\mathrm{Li}}_{\mathrm{DIS}}}{C^{^7\mathrm{Li}}_{\mathrm{JCC}}}}{X_{\mathrm{DIS}}\dfrac{C^{^6\mathrm{Li}}_{\mathrm{DIS}}}{C^{^6\mathrm{Li}}_{\mathrm{JCC}}}}=\frac{\dfrac{C^{^7\mathrm{Li}}_{\mathrm{RIV}}}{C^{^7\mathrm{Li}}_{\mathrm{JCC}}}}{\dfrac{C^{^6\mathrm{Li}}_{\mathrm{RIV}}}{C^{^6\mathrm{Li}}_{\mathrm{JCC}}}}=\frac{\dfrac{C^{^7\mathrm{Li}}_{\mathrm{RIV}}}{C^{^6\mathrm{Li}}_{\mathrm{RIV}}}}{\dfrac{C^{^7\mathrm{Li}}_{\mathrm{JCC}}}{C^{^6\mathrm{Li}}_{\mathrm{JCC}}}} \qquad [4]$$

Equation **3** can now be expressed in terms of both ^{7}Li and ^{6}Li and, according to assumption two, the ratio of these two equations should be related to the lithium isotopic composition of modern rivers (RIV), so we have

$$\frac{\dfrac{C^{^7\mathrm{Li}}_{\mathrm{RIV}}}{C^{^6\mathrm{Li}}_{\mathrm{RIV}}}}{\dfrac{C^{^7\mathrm{Li}}_{\mathrm{JCC}}}{C^{^6\mathrm{Li}}_{\mathrm{JCC}}}}=\frac{1-X_{\mathrm{BCC}}\dfrac{C^{^7\mathrm{Li}}_{\mathrm{BCC}}+R_{\mathrm{RLC/BCC}}C^{^7\mathrm{Li}}_{\mathrm{RLC}}+R_{\mathrm{TER/BCC}}C^{^7\mathrm{Li}}_{\mathrm{TER}}}{C^{^7\mathrm{Li}}_{\mathrm{JCC}}}}{1-X_{\mathrm{BCC}}\dfrac{C^{^6\mathrm{Li}}_{\mathrm{BCC}}+R_{\mathrm{RLC/BCC}}C^{^6\mathrm{Li}}_{\mathrm{RLC}}+R_{\mathrm{TER/BCC}}C^{^6\mathrm{Li}}_{\mathrm{TER}}}{C^{^6\mathrm{Li}}_{\mathrm{JCC}}}} \qquad [5]$$

We use the world river data compilation of Huh et al. (23), who report that the discharge-weighted average Li concentration is 1.5 ppb and δ^7Li is +23.4‰. These values are adopted for the soluble component that is removed from the continents during chemical weathering (DIS) over the course of Earth history. Then the only remaining unknown, X_{BCC}, can be solved using data from Table 2, providing that the ratio by mass of recycled lower crust compared to the mass of BCC ($R_{\mathrm{RLC/BCC}}$) and the ratio by mass of terrigenous sediment removed by subduction compared to the mass of BCC ($R_{\mathrm{TER/BCC}}$) are assumed. Based on studies from the Sierra Nevada Batholith, which represents a Cretaceous continental arc in California, USA (44, 45), $R_{\mathrm{RLC/BCC}}=X_{\mathrm{RLC}}/X_{\mathrm{BCC}}=1$. $R_{\mathrm{TER/BCC}}$ can be calculated from the average modern subducted sediment flux. Global subducted sediment flux has been estimated by various methods, including O and Nd isotopes, and sedimentary records from deep sea drilling projects (41, 46–50), and varies from 1.1×10^{12} to 4.4×10^{12} kg/y, assuming the average density of the subducted sediments is 2.65 g/cm^3 (46). Thus, $R_{\mathrm{TER/BCC}}=0.33$, assuming that the average subducted sediment flux is constant through time at 2.1×10^{12} kg/y and continental crust formed since 3.5 Ga, approximately the start of the geologic record (see (37), and references therein). Below, we evaluate how changing the input parameters affects the outcome of the model.

Results and Uncertainties

Using the above assumptions and inputs for scenario one, the calculated X_{BCC} is 0.17. Therefore, the mass fraction of BCC and RLC are both 17%, and the mass fraction lost to chemical weathering (X_{DIS}) is 60%. For scenario two, the mass fraction of BCC and RLC are both 24%, and the mass fraction lost to chemical weathering (X_{DIS}) is 43%. Both results are displayed in Fig. 3.

We performed sensitivity analyses to evaluate which of the input parameters have the greatest influence on the results and whether it is possible for X_{DIS} to equal zero. The simplest form of sensitivity analysis is the one-at-a-time measure (51), which repeatedly varies one parameter at a time while keeping others constant. A simple way to quantitatively determine the sensitivity of different parameters is to calculate the relative difference of output between maximum and minimum values of the varying parameters (51). The sensitivity index, defined as $\mathrm{SI}=\frac{X_{\max}-X_{\min}}{X_{\max}}$, was calculated for each series of the input parameters. The results are provided in Table 2 (see Dataset S3 for details) and are discussed below.

For the crustal input, $C^{\mathrm{Li}}_{\mathrm{JCC}}$ for scenario one was allowed to vary from 4.5 to 10.6 ppm and δ^7Li values from +2.4‰ to +4.8‰

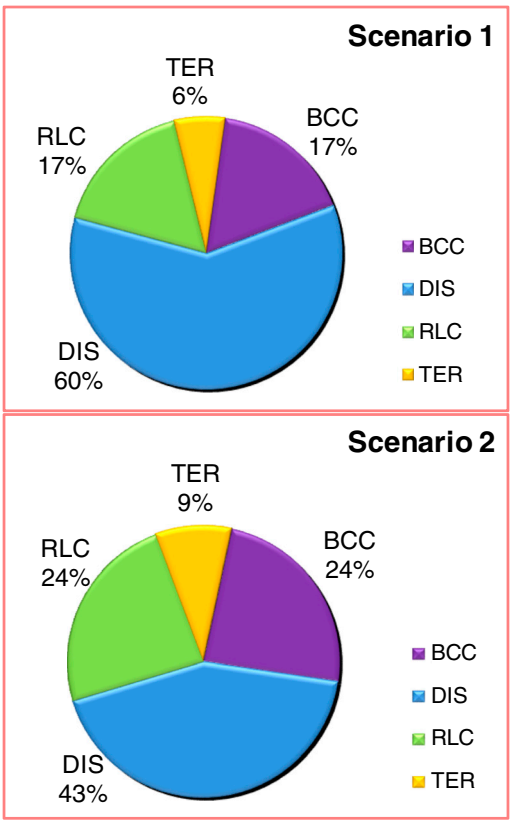

Fig. 3. Pie diagrams of the optimal model results for two end-member scenarios, illustrating different portions of crustal types that must be added together to equal the juvenile continental crust.

(the one sigma seen in arc basalts) during the parameter sensitivity analysis. For scenario two, JCC concentration was allowed to vary from 8 to 14 ppm and δ^7Li values from +3.4‰ to +4.5‰ (see above discussion); a discussion of the constraints on the proportion of primary TTG in the continental crust, which strongly influences the Li concentration in scenario two, is provided in the next section, along with consideration of the influence of using other types of primary basalt for the basaltic component of JCC. For BCC, Li concentration was allowed to range from 11 to 20 ppm, based on the range of published values (1 and references therein). The optimal δ^7Li of the BCC (+1.2‰) was calculated based on weighted δ^7Li of the upper, middle, and lower crust, with their corresponding weight proportions of 0.32:0.29:0.39 (1, 52). However, there are uncertainties associated with Li concentrations and δ^7Li of each crustal layer. Keeping the optimal Li concentration estimates for each crustal layer from Teng et al. (17, 24) and using their estimated δ^7Li uncertainty, we can propagate the uncertainty for δ^7Li in each layer and calculate the weighted δ^7Li of the BCC, which is +1.2‰ ± 5 (1σ). However, the δ^7Li of BCC is unlikely to be lower than that of the upper continental crust (UCC) or higher than that of the mantle. Therefore, we allowed δ^7Li of the BCC to vary from 0‰ (UCC average) (17) to +4‰ (mantle average) (53, 54, and references therein).

Li concentration of RLC was allowed to vary between the concentration of the mantle (1.5 ppm, 55) and the lower continental crust (8 ppm) (24, 40). δ^7Li of RLC was estimated from analyses of eight granulite xenoliths reported in Teng et al. (24), with a concentration-weighted average value of +2.5‰ and a simple average of +1.6‰ ± 8.9 (1σ). Although δ^7Li values vary from −14‰ to +14.3‰ in granulite xenoliths, the isotopic heterogeneity of many of these samples was interpreted by Teng et al. (2008) to reflect the combined effects of isotopic fractionation during prograde metamorphism and kinetic Li isotopic fractionation associated with basaltic intrusions. Recent results for granulite-facies metapelites and metabasites from the Ivrea-Verbano Zone, Italy, suggest a concentration-weighted average δ^7Li of the lower crust in this region of 1.0‰ (40). Nonetheless, the average δ^7Li value of RLC is allowed to vary from −7.5‰ to +11.5‰ for the sensitivity analysis, based on the one-sigma variation in δ^7Li from the eight granulite xenoliths studied by Teng et al. (24) (i.e., +2.5‰ ± 9).

A new estimate of global subducting sediment (GLOSS-II) reports Li concentration of 45 ± 3 ppm (42); δ^7Li of terrigenous turbidities and pelagic clays vary from −1.6‰ to +5‰ (43). However, GLOSS includes chemical and biogenic sediments, such as porcellanite, chert, ooze, radiolarite, and chalk, and it may therefore not reflect pure terrigenous Li values. Compiled Li concentrations of terrigenous sediments using recent ICP-MS data yield an average Li concentration of 48 ppm in TER, with lower and upper limits of 32 ppm and 73 ppm (1σ), respectively (Dataset S1). Therefore, we adopt values for TER ranging from 32 to 73 ppm and −1.6‰ to +5‰ in the sensitivity analysis. The δ^7Li values for individual rivers range from +6.0‰ (23) to +43.7‰ (21). Our compilation of Li isotopic compositions in rivers (Dataset S1) shows an average δ^7Li of +21‰ ± 7 (1σ). Thus, δ^7Li values varying from +14‰ to +28‰ were used for the parameter sensitivity analysis.

Of all the input parameters tested, X_{DIS} is most sensitive to the Li concentration adopted for JCC and BCC. For example, in scenario two, allowing Li concentration in JCC to vary within the one-sigma limits results in the largest range in X_{DIS}, from 22% to 56%. Similarly, allowing the Li concentration in BCC to vary within different authors' estimates (see 1, and references therein), results in a relatively large range in X_{DIS}, from 31% to 47% (see Table 2 and Dataset S3 for details).

Only one mass fraction ratio of RLC to BCC ($R_{RLC/BCC} = 1$) is considered in the mass balance model. In the limiting case of no lower crustal recycling, $R_{RLC/BCC} = 0$, we obtain $X_{DIS} = 75\%$ and 63%, for scenarios one and two, respectively. However, we consider this case to be unlikely, based on evidence from a variety of Phanerozoic settings for such recycling (see summary in 56). Furthermore, according to Plank (57), 25–60% of the JCC ($X_{RLC} = 25$–60%) is lost due to foundering of mafic cumulates and restites, which corresponds to a range of $R_{RLC/BCC}$ from 1 to 4 and X_{DIS} of 23 to 53% and 14 to 43% for scenarios one and two, respectively. The latter provides the minimum estimate of X_{DIS} for any of the various outcomes (Table 2).

Proportion of Tonalite-Trondhjemite-Granodiorite in Juvenile Continental Crust

The above exercise evaluates the uncertainties in the mass balance calculation and identifies the most important parameters (i.e., Li concentration in JCC and BCC) that control the calculated continental crustal mass loss due to weathering, assuming that ≤30% of JCC comprises Archean TTG. Here we evaluate the bounds that can be placed on the proportion of TTG in JCC and how these bounds influence the weathering outcome. Since the mass lost due to weathering decreases with increasing proportion of TTG in juvenile crust, it is important to obtain a robust estimate of the maximum proportion of juvenile TTG in the crust in order to determine the minimum mass lost due to weathering.

We assume that addition of juvenile TTG is primarily confined to the Archean (e.g., 11), so a first step in placing bounds on the juvenile TTG component is to estimate the amount of present-day continental crust that formed in the Archean. Based on global geological maps, Goodwin (58) estimated that Archean crust comprises 7% of total crust. Such an estimate is certainly a minimum, as Archean crust is often reworked by later events. A recent compilation of Lu-Hf model ages in detrital zircon suggests that Archean crust may constitute up to 60% of the present continental crust (59, and references therein), an estimate that coincides with the previous estimate of Taylor and McLennan (36). Given that Archean cratons are generally regions of low surface heat flow (60), these data, coupled with heat production for typical TTG and arc basalt, can be used to estimate the proportion of Archean crust that is TTG. A 40 km thick crust (61) composed of average Archean TTG of Condie (62) would produce a surface heat flow of 44.3 mW/m^2, whereas 40 km of average arc basalt (63) generates a surface heat flow of 12.4 mW/m^2. Given that the average heat flow in Archean crust is 41 mW/m^2 (64) and the minimum Moho heat flux is estimated to be 11 mW/m^2 (60), the maximum surface heat flux generated in average Archean crust is 29 mW/m^2, which places an upper limit on the proportion of TTG in Archean continental crust of ~55%. Combined with the limits discussed above, we estimate that the percentage of TTG in the entire juvenile crust can range from 4% to 33%. Therefore, even in the extreme case, where 33% of the JCC is composed of Archean TTG, yielding a Li concentration of 15 ppm for JCC, the weathering mass loss is still ~25% of total juvenile continental crust. The proportion of Archean TTG would need to rise to 59% of the mass of the JCC in order for the weathering mass flux to drop to zero. However, such a large mass fraction of TTG is unlikely, given geological constraints.

The Juvenile Basaltic Crust

We have chosen average modern arc basalt as the juvenile basaltic end member. How might the picture change if other types of basalts are considered instead, since subducted terrigenous sediments may influence the Li composition of arc basalt (42)? Data for Li in MORB compiled from PetDB (65), supplemented with data from recent Li isotope studies (54, 66) and Li in OIB from the GEOROC (35) database, are reported in the Dataset S2 and shown in Fig. 4. Like arc basalts, Li concentrations in both MORB and OIB follow log-normal distributions, having means of

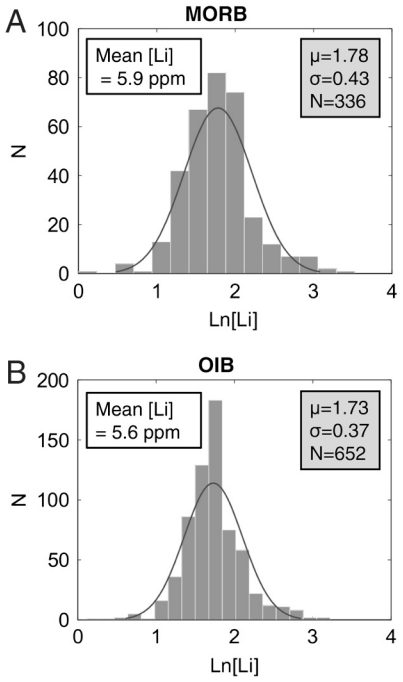

Fig. 4. Histogram of lithium concentrations in MORB and OIB. μ, σ, and N represent mean, standard deviation, and number of the sample population. (*A*) In MORB, Li concentration follows a log-normal (natural log) distribution with a mean of 5.9 ppm and upper and lower limits of 9.1 ppm and 3.9 ppm, respectively. (*B*) In OIB, Li concentration follows a log-normal (natural log) distribution with a mean of 5.6 ppm and upper and lower limits of 8.2 ppm and 3.9 ppm, respectively.

5.9 and 5.6 ppm, respectively, which are slightly lower compared to the mean of arc basalts, 6.9 ppm. The slight enrichment of Li seen in arc basalts is likely due to incorporation of Li from subducted sediments (42). In this sense, Li lost from the continental crust in TER, partially reenters the crust in arc basalts. Thus, using arc basalt for the JCC rather than MORB or OIB accounts for this Li "short circuit." Perhaps more importantly, during the sensitivity test discussed above, Li concentration in JCC was allowed to be as low as 4.5 ppm, which encompasses the mean Li concentrations of MORB and OIB. Therefore, the choice of basaltic source does not significantly influence the mass balance model.

In summary, the global uncertainty (accounting for variations in all parameters) in the mass balance model is large. However, even with these uncertainties, we show that a considerable mass (at least 15%, with a best estimate of approximately 45%) of the juvenile continental crust was lost via incongruent chemical weathering, given the best available constraints on the input parameters in this first-order mass balance model.

Model Predictions and Discussion

We show that zero mass loss due to chemical weathering is not a possible outcome, which is consistent with observations from other stable isotope systems, such as oxygen (47), that the bulk continental crust is isotopically distinct from the mantle due to the cumulative effects of chemical weathering over Earth history. Chemical weathering is one of the mechanisms that preferentially removes soluble elements, such as magnesium—abundant in easily weathered mafic minerals (e.g., olivine and pyroxene), and leaves silicon- and aluminum-rich, weathering-resistant minerals (e.g., quartz and clays). Therefore, the mass balance model and its accompanying uncertainty estimates indicate that chemical weathering plays an important role in shifting the continental crust composition from basaltic ($SiO_2 = 45 \sim 55$ wt. %) to andesitic ($SiO_2 = 57 \sim 64$ wt. %). This quantification of the amount of chemical weathering mass loss (>15%) over geological history is consistent with the 20% of chemical weathering mass loss suggested by Lee et al. (6), and provides a first-order constraint for further investigation of the crust composition paradox.

Important predictions from this study also include total mass of dissolved continental crust (ultimately subducted in altered oceanic crust), total mass of continental crust subducted as terrigneous sediments, and total mass of continental crust formed over Earth's history, all of which are shown in Table 3 for scenarios one and two. We calculate the mass ratio of different components relative to the BCC. The mass of dissolved continental crust is four and two times that of the mass of BCC for scenarios one and two, respectively, while the total mass of the juvenile continental crust (JCC) is six and four times that of BCC for scenarios one and two, respectively. Interestingly, both the mass of dissolved continental crust and total mass of juvenile continental crust in scenario two are twice as much as those in scenario one, although the mass of continental crust (TER) is about 30% of the mass of BCC in both scenarios.

The results from this study can also be used to estimate the global average chemical weathering rate over Earth history. The minimum current chemical weathering rate estimated from dissolved material originating from rock weathering in the 60 largest rivers on Earth is about 2.1×10^9 t/y (67). This estimate does not incorporate weathering of basalts in arcs, where the chemical weathering rate is higher compared to the average continental silicate weathering rate (e.g., 68, 69); it also does not include the dissolved continental material lost via groundwater flow into the oceans, which may be as much as 50% of that contributed by rivers (70), although the overall flow of groundwater into the ocean is not likely to be more than 6% of the total continental runoff (71). Thus, this chemical weathering rate estimate is considered a minimum estimate. The mass of the current bulk continental crust, M_{BCC}, is $\sim 2.2 \times 10^{22}$ kg (72). The optimal X_{DIS} varies between 43% ($X_{BCC} = 24\%$) and 60% ($X_{BCC} = 17\%$) for scenario two and one, respectively; the mass lost during chemical weathering, M_{DIS}, can be estimated from X_{DIS}/X_{BCC}. If we assume that the continental crust has mainly formed since 3.5 Ga, then the average global chemical weathering rate (CWR) can be calculated as approximately 1.1×10^{10} to 2.2×10^{10} t/y, for scenarios two and one, respectively. The choice of age of the continental crust does not significantly influence this outcome. For example, if we assume crust formed mainly since 4.5 Ga or 2.7 Ga, the average CWR will change to approximately 0.9×10^{10} and approximately 1.5×10^{10} t/y, respectively, for the optimal va-

Table 3. Predictions from this study

	Scenario 1	Scenario 2		Scenario 1	Scenario 2
M_{DIS}, kg	7.8×10^{22}	3.9×10^{22}	M_{DIS}/M_{BCC}	4	2
M_{TER}, kg	7.8×10^{21}	8.3×10^{21}	M_{TER}/M_{BCC}	0.4	0.4
M_{JCC}, kg	1.3×10^{23}	9.2×10^{22}	M_{JCC}/M_{BCC}	6	4
CWR, kg/y	2.2×10^{13}	1.1×10^{13}			

Note: $M_{BCC} = M_{RLC} = 2.2 \times 10^{22}$ kg is used for the above calculations. M_{DIS} is total mass of dissolved continental crust, M_{TER} is total mass of subducted continental crust, M_{JCC} is total mass of continental crust formed over geologic time, and CWR is predicted average chemical weathering rates over time.

lues in scenario two. This range is up to an order of magnitude higher than the estimate of the minimum present-day weathering rate from Gaillardet et al. (67) and may reflect the greater weathering rate in basaltic arcs, continental dissolved mass transported by groundwater and/or an increased weathering rate in the past.

Finally, the assumption that the Li isotopic composition of material removed from the continent due to chemical weathering can be represented by modern rivers may not be valid. Li weathering fluxes from rivers may have changed over the Cenozoic, according to Li isotope studies on forams (73, 74). However, the influence of δ^7Li_{DIS} on the model output is relatively small, and so large changes in the riverine isotopic composition are unlikely to significantly affect the outcome (e.g., in scenario two, if δ^7Li_{DIS} is lower by 9‰, the average river water δ^7Li_{DIS} decreases from the present-day average 23‰ to 14‰, and X_{DIS} increases from 43% to 47%).

Conclusions

Using Li concentration and isotope data in a mass balance model, a significant percentage (at least 15%, with best estimate of approximately 45%) of the juvenile continental crustal mass is found to be lost from the continents due to chemical weathering. The mass balance model is particularly sensitive to the composition of primary crustal additions. The accumulated percentage of mass loss due to chemical weathering leads to an average global chemical weathering rate (CWR) of approximately 9×10^9 to approximately 2×10^{10} t/y since 3.5 Ga, which is about an order of magnitude higher than the current (minimum) estimates based on modern rivers. While we cannot constrain the exact portion of crustal mass loss via chemical weathering, given the uncertainties of the calculation, we can demonstrate that the weathering flux is nonzero. Therefore, chemical weathering must play a role in the evolution of the composition and mass of the continental crust.

AKNOWLEDGMENTS. Discussions with Mike Evans, Bill McDonough, and Lin Qiu and review comments of Steve Goldstein, Cin-Ty Lee, Romain Millot, Hugh Rollinson, and an anonymous reviewer on an earlier draft helped us to strengthen the paper. This work was supported by funding from the National Science Foundation (Grants EAR 0609689 and EAR 0948549).

1. Rudnick RL, Gao S (2003) Composition of the continental crust. *The Crust*, ed RL Rudnick (Elsevier-Pergamon, Oxford), *Treatise on Geochemistry*, eds HD Holland, KK Turekian, Vol 3, pp 1–64.
2. Rudnick RL (1995) Making Continental Crust. *Nature* 378:571–578.
3. Rollinson H (2008) Secular evolution of the continental crust: Implications for crust evolution models. *Geochem Geophys Geosyst* 9:Q12010.
4. Anderson AT (1982) Parental basalts in subduction zones—implications for continental evolution. *J Geophys Res* 87:7047–7060.
5. Albarede F (1998) The growth of continental crust. *Tectonophysics* 296:1–14.
6. Lee CTA, et al. (2008) Regulating continent growth and composition by chemical weathering. *Proc Natl Acad Sci USA* 105:4981–4986.
7. Jull M, Kelemen PB (2001) On the conditions for lower crustal convective instability. *J Geophys Res-Sol Ea* 106:6423–6446.
8. Arndt NT, Goldstein SL (1989) An open boundary between lower continental crust and mantle: its role in crust formation and crustal recycling. *Tectonophysics* 161: 201–212.
9. Kay RW, Mahlburg Kay S (1993) Delamination and delamination magmatism. *Tectonophysics* 219:177–189.
10. Hacker BR, Kelemen PB, Behn MD (2011) Differentiation of the continental crust by relamination. *Earth Planet Sci Lett* 307:501–516.
11. Martin H (1986) Effect of steeper Archean geothermal gradient on geochemistry of subduction-zone magmas. *Geology* 14:753–756.
12. Tomascak PB (2004) Developments in the understanding and application of lithium isotopes in the earth and planetary sciences. *Geochemistry of Non-Traditional Stable Isotopes*, eds CM Johnson, BL Beard, and F Albarede Vol 55 (Mineralogical Society of America, Washington, D.C.), 153–195 Reviews in Mineralogy & Geochemistry.
13. Flesch G, Anderson A, Svec H (1973) A secondary isotopic standard for $^6Li/^7Li$ determinations. *Int J Mass Spectrom* 12:265–272.
14. Huh Y, Chan LH, Edmond JM (2001) Lithium isotopes as a probe of weathering processes: Orinoco River. *Earth Planet Sci Lett* 194:189–199.
15. Huh Y, Chan L-H, Chadwick OA (2004) Behavior of lithium and its isotopes during weathering of Hawaiian basalt. *Geochem Geophys Geosyst* 5:Q09002.
16. Kisakurek B, Widdowson M, James RH (2004) Behaviour of Li isotopes during continental weathering: the Bidar laterite profile, India. *Chem Geol* 212:27–44.
17. Teng FZ, et al. (2004) Lithium isotopic composition and concentration of the upper continental crust. *Geochim Cosmochim Ac* 68:4167–4178.
18. Pistiner JS, Henderson GM (2003) Lithium-isotope fractionation during continental weathering processes. *Earth Planet Sci Lett* 214:327–339.
19. Millot R, Vigier N, Gaillardet J (2010) Behaviour of lithium and its isotopes during weathering in the Mackenzie Basin, Canada. *Geochim Cosmochim Ac* 74:3897–3912.
20. Vigier N, Gislason SR, Burton KW, Millot R, Mokadem F (2009) The relationship between riverine lithium isotope composition and silicate weathering rates in Iceland. *Earth Planet Sci Lett* 287:434–441.
21. Pogge von Strandmann PAE, et al. (2006) Riverine behaviour of uranium and lithium isotopes in an actively glaciated basaltic terrain. *Earth Planet Sci Lett* 251:134–147.
22. Wimpenny J, et al. (2010) Glacial effects on weathering processes: New insights from the elemental and lithium isotopic composition of West Greenland rivers. *Earth Planet Sci Lett* 290:427–437.
23. Huh Y, Chan LH, Zhang L, Edmond JM (1998) Lithium and its isotopes in major world rivers: Implications for weathering and the oceanic budget. *Geochim Cosmochim Ac* 62:2039–2051.
24. Teng FZ, et al. (2008) Lithium isotopic composition and concentration of the deep continental crust. *Chem Geol* 255:47–59.
25. Pogge von Strandmann PAE, Burton KW, James RH, van Calsteren P, Gislason SR (2010) Assessing the role of climate on uranium and lithium isotope behaviour in rivers draining a basaltic terrain. *Chem Geol* 270:227–239.
26. Pogge von Strandmann PAE, James RH, van Calsteren P, Gislason SR, Burton KW (2008) Lithium, magnesium and uranium isotope behaviour in the estuarine environment of basaltic islands. *Earth Planet Sci Lett* 274:462–471.
27. Martin H, Moyen JF (2002) Secular changes in tonalite-trondhjemite-granodiorite composition as markers of the progressive cooling of Earth. *Geology* 30:319–322.
28. Tomascak PB, Widom E, Benton LD, Goldstein SL, Ryan JG (2002) The control of lithium budgets in island arcs. *Earth Planet Sci Lett* 196:227–238.
29. Moriguti T, Nakamura E (1998) Across-arc variation of Li isotopes in lavas and implications for crust/mantle recycling at subduction zones. *Earth Planet Sci Lett* 163:167–174.
30. Moriguti T, Shibata T, Nakamura E (2004) Lithium, boron and lead isotope and trace element systematics of Quaternary basaltic volcanic rocks in northeastern Japan: mineralogical controls on slab-derived fluid composition. *Chem Geol* 212:81–100.
31. Chan LH, Leeman WP, You CF (2002) Lithium isotopic composition of Central American volcanic arc lavas: implications for modification of subarc mantle by slab-derived fluids: correction. *Chem Geol* 182:293–300.
32. Ryan JG, Kyle PR (2004) Lithium abundance and lithium isotope variations in mantle sources: insights from intraplate volcanic rocks from Ross Island and Marie Byrd Land (Antarctica) and other oceanic islands. *Chem Geol* 212:125–142.
33. Qiu L (2011) Lithium and δ^7Li Behavior During Metamorphic Dehydration Processes and Crustal Evolution. PhD thesis (University of Maryland).
34. Magna T, Wiechert U, Grove TL, Halliday AN (2006) Lithium isotope fractionation in the southern Cascadia subduction zone. *Earth Planet Sci Lett* 250:428–443.
35. GEOROC, (http://georoc.mpch-mainz.gwdg.de/georoc/) (accessed July 2011).
36. Taylor SR, McLennan SM (2009) *Planetary crusts: their composition, origin and evolution* (Cambridge Univ Press, Cambridge, UK).
37. Kemp AIS, Hawkesworth CJ (2012) Growth and differentiation of the continental crust from isotope studies of accessory minerals. *The Crust*, ed RL Rudnick (Elsevier-Pergamon, Oxford), in press, *Treatise on Geochemistry*, eds HD Holland, KK Turekian, 2nd Ed, Vol 4.
38. Shirey SB, Hanson GN (1984) Mantle-derived Archean monzodiorites and trachyandesites. *Nature* 310:222–224.
39. Clemens JD, Yearron LM, Stevens G (2006) Barberton (South Africa) TTG magmas: Geochemical and experimental constraints on source-rock petrology, pressure of formation and tectonic setting. *Precambrian Res* 151:53–78.
40. Qiu L, Rudnick RL, McDonough WF, Bea F (2011) The behavior of lithium in amphibolite- to granulite-facies rocks of the Ivrea—Verbano Zone NW Italy. *Chem Geol* 289:76–85.
41. Albarede F (1989) Sm-Nd Constraints on the growth rate of continental crust. *Tectonophysics* 161:299–305.
42. Plank T (2012) The chemical composition of subducting sediments, pp. *The Crust*, ed RL Rudnick (Elsevier-Pergamon, Oxford), in press, *Treatise on Geochemistry*, eds HD Holland, KK Turekian, 2nd Ed, Vol 4.
43. Chan L-H, Leeman WP, Plank T (2006) Lithium isotopic composition of marine sediments. *Geochem Geophys Geosyst* 7:Q06005.
44. Lee CTA, Cheng X, Horodyskyj U (2006) The development and refinement of continental arcs by primary basaltic magmatism, garnet pyroxenite accumulation, basaltic recharge and delamination: insights from the Sierra Nevada, California. *Contrib Mineral Petr* 151:222–242.
45. Lee CTA, Morton DM, Kistler RW, Baird AK (2007) Petrology and tectonics of Phanerozoic continent formation: From island arcs to accretion and continental arc magmatism. *Earth Planet Sci Lett* 263:370–387.
46. Rea DK, Ruff LJ (1996) Composition and mass flux of sediment entering the world's subduction zones: Implications for global sediment budgets, great earthquakes, and volcanism. *Earth Planet Sci Lett* 140:1–12.
47. Simon L, Lécuyer C (2005) Continental recycling: The oxygen isotope point of view. *Geochem Geophys Geosyst* 6:Q08004.
48. Plank T, Langmuir CH (1998) The chemical composition of subducting sediment and its consequences for the crust and mantle. *Chem Geol* 145:325–394.
49. Depaolo DJ (1983) The mean life of continents—Esimates of continent recycling rates from Nd and Hf isotopic data and implications for mantle structure. *Geophys Res Lett* 10:705–708.

50. Clift PD, Vannucchi P, Morgan JP (2009) Crustal redistribution, crust-mantle recycling and Phanerozoic evolution of the continental crust. *Earth-Science Reviews* 97: 80–104.
51. Hamby DM (1994) A Review of Techniques of Parameter Sensitivity Analysis of Environmental Models. *Environ Monit Assess* 32:135–154.
52. Rudnick RL, Fountain DM (1995) Nature and composition of the continental crust—A lower crustal perspective. *Rev Geophys* 33:267–309.
53. Pogge von Strandmann PAE, et al. (2011) Variations of Li and Mg isotope ratios in bulk chondrites and mantle xenoliths. *Geochim Cosmochim Ac* 75:5247–5268.
54. Tomascak PB, Langmuir CH, le Roux PJ, Shirey SB (2008) Lithium isotopes in global mid-ocean ridge basalts. *Geochim Cosmochim Ac* 72:1626–1637.
55. McDonough WF, Sun SS (1995) The composition of the earth. *Chem Geol* 120: 223–253.
56. Lee CTA (2012) Physics and chemistry of deep continental crust recycling. *The Crust*, ed RL Rudnick (Elsevier-Pergamon, Oxford), in press, *Treatise on Geochemistry*, eds HD Holland, KK Turekian, 2nd Ed, Vol 4.
57. Plank T (2005) Constraints from thorium/lanthanum on sediment recycling at subduction zones and the evolution of the continents. *J Petrol* 46:921–944.
58. Goodwin AM (1996) *Principles of Precambrian geology* (Academic, New York), 2nd edition.
59. Belousova EA, et al. (2010) The growth of the continental crust: Constraints from zircon Hf-isotope data. *Lithos* 119:457–466.
60. Jaupart C, Mareschal JC (2012) Constraints on crustal heat production from heat flow data. *The Crust*, ed RL Rudnick (Elsevier-Pergamon, Oxford), in press, *Treatise on Geochemistry*, eds HD Holland, KK Turekian, 2nd Ed, Vol 4.
61. Christensen NI, Mooney WD (1995) Seismic velocity structure and composition of the continental crust: A global view. *J Geophys Res* 100:9761–9788.
62. Condie KC (2005) TTGs and adakites: are they both slab melts? *Lithos* 80:33–44.
63. Kelemen PB, Hanghøj K, Greene AR (2007) One view of the geochemistry of subduction-related magmatic arcs, with an emphasis on primitive andesite and lower crust. *The Crust*, ed RL Rudnick (Elsevier-Pergamon, Oxford), *Treatise on Geochemistry*, eds HD Holland, KK Turekian, Vol 3, pp 1–70.
64. Nyblade AA, Pollack HN (1993) A Global Analysis of Heat Flow From Precambrian Terrains: Implications for the Thermal Structure of Archean and Proterozoic Lithosphere. *J Geophys Res* 98:12207–12218.
65. PetDB, (http://www.petdb.org/) (accessed July 2011).
66. Elliott T, Thomas A, Jeffcoate A, Niu YL (2006) Lithium isotope evidence for subduction-enriched mantle in the source of mid-ocean-ridge basalts. *Nature* 443: 565–568.
67. Gaillardet J, Dupre B, Louvat P, Allegre CJ (1999) Global silicate weathering and CO2 consumption rates deduced from the chemistry of large rivers. *Chem Geol* 159:3–30.
68. Louvat P, Allegre CJ (1997) Present denudation rates on the island of Reunion determined by river geochemistry: Basalt weathering and mass budget between chemical and mechanical erosions. *Geochim Cosmochim Ac* 61:3645–3669.
69. Dessert C, et al. (2001) Erosion of Deccan Traps determined by river geochemistry: impact on the global climate and the Sr-87/Sr-86 ratio of seawater. *Earth Planet Sci Lett* 188:459–474.
70. Zektser IS, Loaiciga HA (1993) Groundwater fluxes in the global hydrologic-cycle—past, present and future. *J Hydrol* 144:405–427.
71. Burnett WC, Bokuniewicz H, Huettel M, Moore WS, Taniguchi M (2003) Groundwater and pore water inputs to the coastal zone. *Biogeochemistry* 66:3–33.
72. Peterson BT, Depaolo DJ (2007) Mass and composition of the continental crust estimated using the CRUST2.0 model. *Transactions of the American Geophysical Union*, 88 Fall meeting supplement, Abstract V33A-1161.
73. Hathorne EC, James RH (2006) Temporal record of lithium in seawater: A tracer for silicate weathering? *Earth Planet Sci Lett* 246:393–406.
74. Misra S, Froelich PN (2010) Seawater Lithium isotope evolution during the Cenozoic. *Geochim Cosmochim Ac* 74(12, Supplement 1):A713.